Arab J Geosci (2014) 7:3983–3994
DOI 10.1007/s12517-013-1063-6

ORIGINAL PAPER

Identification of fracture development period and stress field analysis based on fracture fabrics in tectonic superposition areas

Nan Su · Lejun Zou · Xiaohua Shen · Wenyuan Wu · Guifang Zhang · Fanli Kong · Zhong Zhang · Youpu Dong · Ancheng Xiao

Received: 12 March 2013 / Accepted: 30 July 2013 / Published online: 11 September 2013

Abstract As a direct consequence of multiple periods of stress applied on areas with tectonic superposition, the multiple-periods fractures have complex abutting relationships, and the field study of fractures is usually restricted by outcrop conditions, such as section direction. Therefore, previous studies of superposed stress fields based on fractures have been generally performed in areas with proper observation conditions and clear abutting relationships. In contrast, in many other areas, the identification of fracture development period based on field observation is often infeasible. Compared to abutting relationships, fracture fabrics obtained from field measurement are not affected by the restriction of outcrops and consequently are more representative of the fractures. According to the analysis of fracture fabrics and fracture features, this paper has separated and extracted the superposed fracture sets and identified the fracture development period in the area without available abutting relationships. Taking the southern segment of the Longmen Mountain thrust belt as an example, fractures of two development periods are identified and timed in the tectonic superposition area between two adjacent fold belts. The analysis of stress direction in each period suggests that the structural boundaries, consisting of such pre-existing structures as faults and anticlines, could have induced directional rotation in the subsequent stress. An equivalent result was achieved using a finite element simulation of the stress field. Based on the stress analysis of the field sites and the stress field simulation, the stress variation in the tectonic superposition area is well modeled.

Keywords Timing of fracture development · Fracture fabrics · Tectonic superposition areas · Stress field · Structural boundary

N. Su · L. Zou · X. Shen (✉) · F. Kong · Z. Zhang · Y. Dong · A. Xiao
Department of Earth Science, Zhejiang University, 223 Room, Teach building 6, 38 Zheda Road, Hangzhou 310027, Zhejiang, China
e-mail: shenxh@zju.edu.cn

W. Wu
Institute of Remote Sensing and Earth Sciences, Hangzhou Normal University, Hangzhou 310036, Zhejiang, China
e-mail: wwyzju@qq.com

G. Zhang
Department of Earth Sciences, Sun Yat-sen University, 135 West Xin-Gang Road, Guangzhou 510275, Guangdong, China
e-mail: zhgfang@mail.sysu.edu.cn

Introduction

The analysis of deformation and stress field in areas with superposition of tectonic events has been discussed much in previous studies because it is one of the most important ways to reveal the evolution of structural history (e.g., Ghosh and Ramberg 1968; Ramsay and Huber 1987; Ghosh et al. 1992). Conferring advantages, such as pervasive development and specific relationships with stress directions, fractures are consequently used in many studies to analyze stress variations (e.g., Memarian and Fergusson 2003; Eyal et al. 2006; Blenkinsop 2008; Diabat 2013). Because stresses with different directions applied on the strata induce various fracture patterns and distribution (Olson 1997, 2003), the fractures developed during structural evolution are complex, but a stress condition always corresponds to a specific fracture pattern. Thus, it is possible to predict the orientation, distribution, and combinations of fractures based on a known stress condition or infer the stress direction based on known fracture patterns. For example, joints are formed perpendicularly to the minimum principal stress and in the plane of the maximum

and intermediate principal stresses; therefore, joints are frequently used to indicate the orientation of the stress field (e.g., Dyer 1988; Pollard and Aydin 1988; Rawnsley et al. 1992).

To analyze the stress fields of multiple periods of deformation, the fracture sets developed in each period should be identified first. In previous studies, the identification of fracture development period was based on the observation of fracture-abutting relationships in the field (e.g., Eyal et al. 2001; Bellahsen et al. 2006). However, some difficulties still exist in areas with complex fractures that inhibit the timing of fractures based on field observations. First, clear abutting relationships often cannot be observed because of poor outcrop conditions, highly fragmented strata, and missing of fracture sets due to the nonuniformity of fracture development and distribution. For example, for bedding-perpendicular fracture sets developed in folds (e.g., Fischer and Wilkerson 2000; Mynatt et al. 2009), it is difficult to determine the abutting relationship in a vertical section perpendicular to the bedding. Second, when dividing fractures into different sets according to field observations, the accuracy is often constrained by the misreading of orientations from individual fractures and by small orientation differences between fracture sets. Therefore, the statistics of a large population of fractures are needed in sets division, but it is difficult to carry out in the field. Third, the development of later fractures may be affected by pre-existing structures or fractures, resulting in a smaller number and shorter lengths of the later fractures. These later fractures are easy to neglect in the field, and consequently the tectonic event that

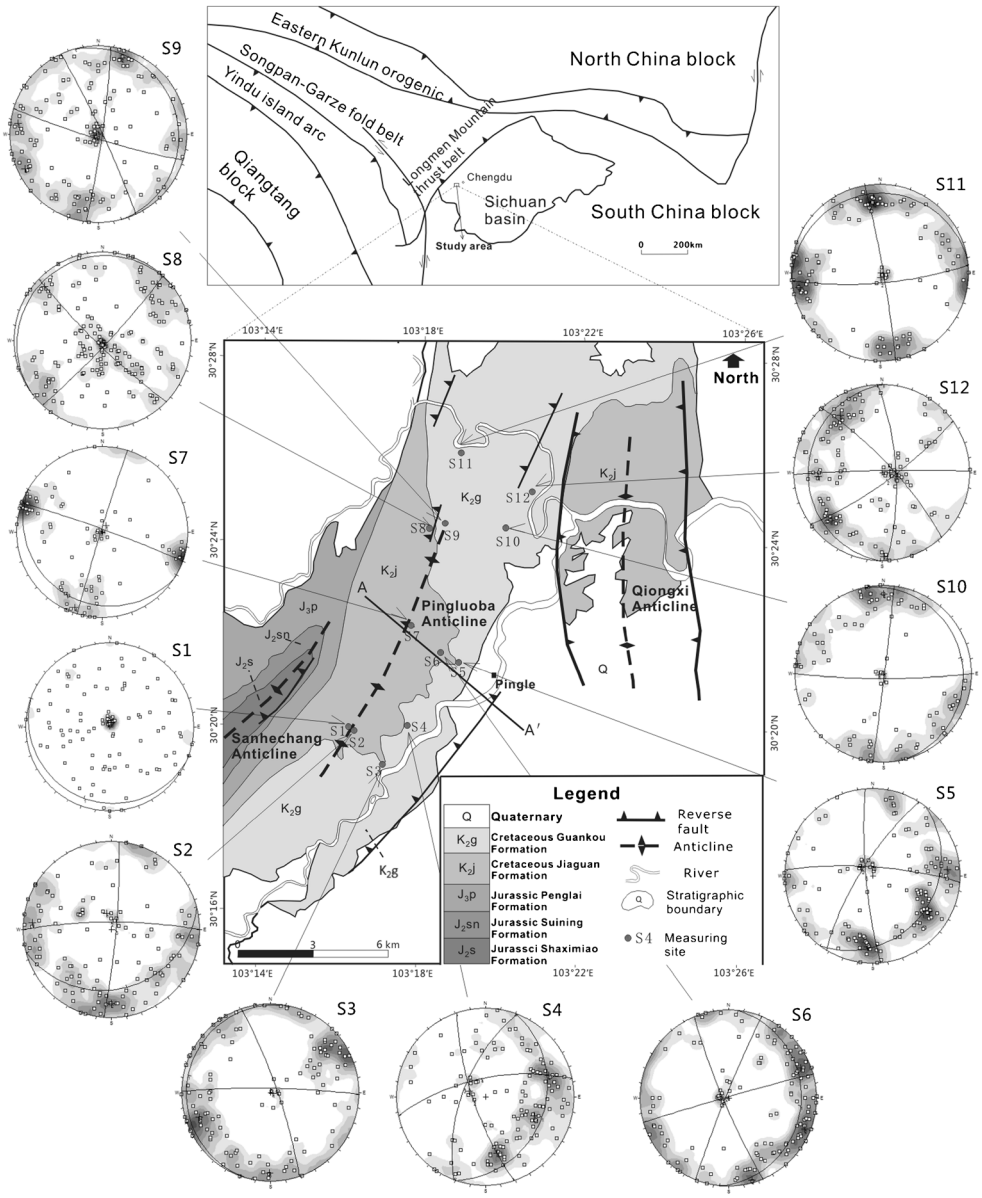

Fig. 1 Geological and tectonic maps of the study area, and the location of a seismic profile in the Pingluoba anticline. The position of each site is marked on the map and the fracture fabrics of each site are shown across the map. *Upper inset* shows the location of the study area in the Longmen Mountain thrust belt

they represent may be overlooked. Therefore, in areas with these difficulties, an improved method is needed to determine the development periods of complex fracture sets.

In this study, we tried to identify the development period of fractures based on an analysis of fracture fabrics. Fracture fabrics (the associative pattern of fracture poles in a contoured polar stereonet) have been used in division of fracture sets and analyses in previous studies (e.g., Ismat and Mitra 2005; Bellahsen et al. 2006). The fracture fabrics obtained from detailed field measurements would tend not to be affected by outcrops conditions. In addition, based on the statistics of fracture orientations, fractures with similar orientations can be divided more accurately into sets and omission of fracture sets which have a small number of fractures can be avoided. Thus, this method is considered more suitable in areas where fractures patterns are complex and clear abutting relationships are difficult to observe.

Study area

The study area is located in the southern segment of the Longmen Mountain thrust belt in the western Sichuan basin, China. The Pingluoba and Qiongxi anticlines are located in the western and eastern regions of the area, respectively (Fig. 1). The Pingluoba anticline belongs to a NNE-striking tectonic belt, which is part of the Longmen Mountain thrust belt; the Qiongxi anticline belongs to an N-striking tectonic belt. The strata in the wide core of the Pingluoba anticline are nearly horizontal, and the strata in the southeast limb have a maximum dip angle of 20°. The deformation of this anticline is controlled by a NE-striking thrust fault in the southeast limb of the anticline. The deformation of the Qiongxi anticline is controlled by two N-striking back-thrust faults, one in each of the two limbs. The two anticlines were developed during different periods. The initial development of the Longmen Mountain thrust belt occurred during the Indo-sinian compression in the late Triassic, whereas the main deformation period of the south segment of the thrust belt, where the study area is located, dates to the late Cretaceous to the early Cenozoic (Jia et al. 2006; Liu 2006; Jin et al. 2010; Deng et al. 2012). Because all the Mesozoic strata are uniformly deformed in the anticline, the deformation of the Pingluoba anticline most likely initiated in the early Cenozoic. The stress direction in the area was consistent in a northwest striking compression from the Indo-sinian period to the early Himalayan period. The deformation of the Qiongxi anticline started after the Pleistocene (Jia et al. 2007; Jia et al. 2009). At that time, the direction of compressive stress, which resulted from the collision of the Indian and Asian plates, was E-W (Dirks et al. 1994; Burchfiel et al. 1995). The principal rock units exposed in the study area, in order of increasing age, are argillaceous sandstones of the Cretaceous Guankou Formation (K_2g), lithic sandstones of the Cretaceous Jiaguan Formation (K_2j), sandy mudstone of Jurassic Penglai Formation (J_3p), mudstone of Jurassic Suining Formation (J_2sn), and conglomerate of Jurassic Shaximiao Formation (J_2s).

Identification of fracture development period based on fracture fabrics

Method

Most outcrops in the study area are vertical sections, and the strata are highly fragmented, with bedding-perpendicular fractures. As a result, the timing of fracture development based on abutting relationships is impossible (Fig. 2a). The data from the measurements of fracture orientations are presented in a contoured polar stereonet on the lower hemisphere, using the equal angle net for further angular analysis, and the fracture poles that concentrate as a cluster (1 % area contour) are considered to constitute a fracture set.

When identifying the fracture development period, fracture sets with similar features in the stereonet, such as the number of poles, concentration and cluster shape, were assumed to have developed in the same period. The predominant fracture sets, i.e., those with the most poles and intense concentration in a given fracture fabrics, were first selected and interpreted as having developed in the same period (Fig. 2b, A). These fractures were then removed from the fracture fabrics, and the remaining fractures were analyzed (Fig. 2b, B). In the removal operation, fractures of the predominant sets were deleted from the original data, and the polar stereonet was regenerated. Fractures whose orientations are nearly parallel to the outcrop were also deleted to avoid any error caused by the measurement. The remaining fracture fabrics at different sites were compared to extract the correlative sets (the sets which could be observed at all these sites), and these sets were interpreted as fractures that developed in another period. These sets were then also deleted to evaluate whether there were additional correlative sets in the remaining fracture fabrics. The deletions and comparisons were repeated because fracture sets with smaller number of fractures were more outstanding and clearer in the stereonet after the deletion of the predominant sets.

The result of development period identification was rechecked based on fracture features including the orientation, extension, distribution, and surface characteristics. Based on similarities and differences between fracture sets that developed in the same period, the possibility of the co-existence of multiple-periods fractures was reexamined. The development sequence of fracture sets during different periods could be determined based on differences in fracture features between the sets. After the development periods of fractures were determined, the stress field of each period in this area could be estimated by correlating the fracture pattern with a compatible stress direction.

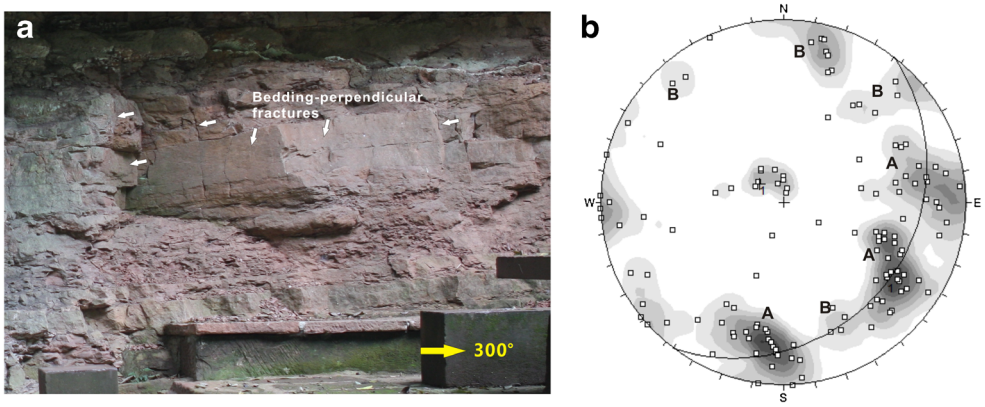

Fig. 2 **a** At S6, fractures which are perpendicular to bedding are mainly developed. The cross-cutting relationships between fractures could not be observed in vertical outcrops. **b** During analysis of fracture fabrics, the predominant fracture sets in the fracture fabrics were first selected (*A*) and then removed to analyze the remaining fractures (*B*)

Twelve sites were measured in detail in the Pingluoba anticline, containing characteristic positions such as fold hinge, limb, and plunging crown (Fig. 1). At each site, 100 to 150 fractures were measured to ensure that the observed fracture data were adequate to reflect the fracture fabrics and include fractures developed during all periods. In the measurement process, the application (software) Sketches, on an iPad tablet, was used to draw distribution maps of all the fractures with their sequence numbers so that they could be located in photos for further analysis.

Fracture fabrics analysis

Based on the fracture fabrics at each site in the study area, three fracture sets are predominant and widely developed (Figs. 1 and 2). The orientations of these fracture sets are consistent at the sites, striking north, east, and northeast. The N- and E-striking sets are developed in the fold hinge, southeast limb, and plunging crown (e.g., S7, S9, S11, and S12), while the northeast-striking set is mainly developed in the southeast limb (S4, S5, and S6). These sets of fractures

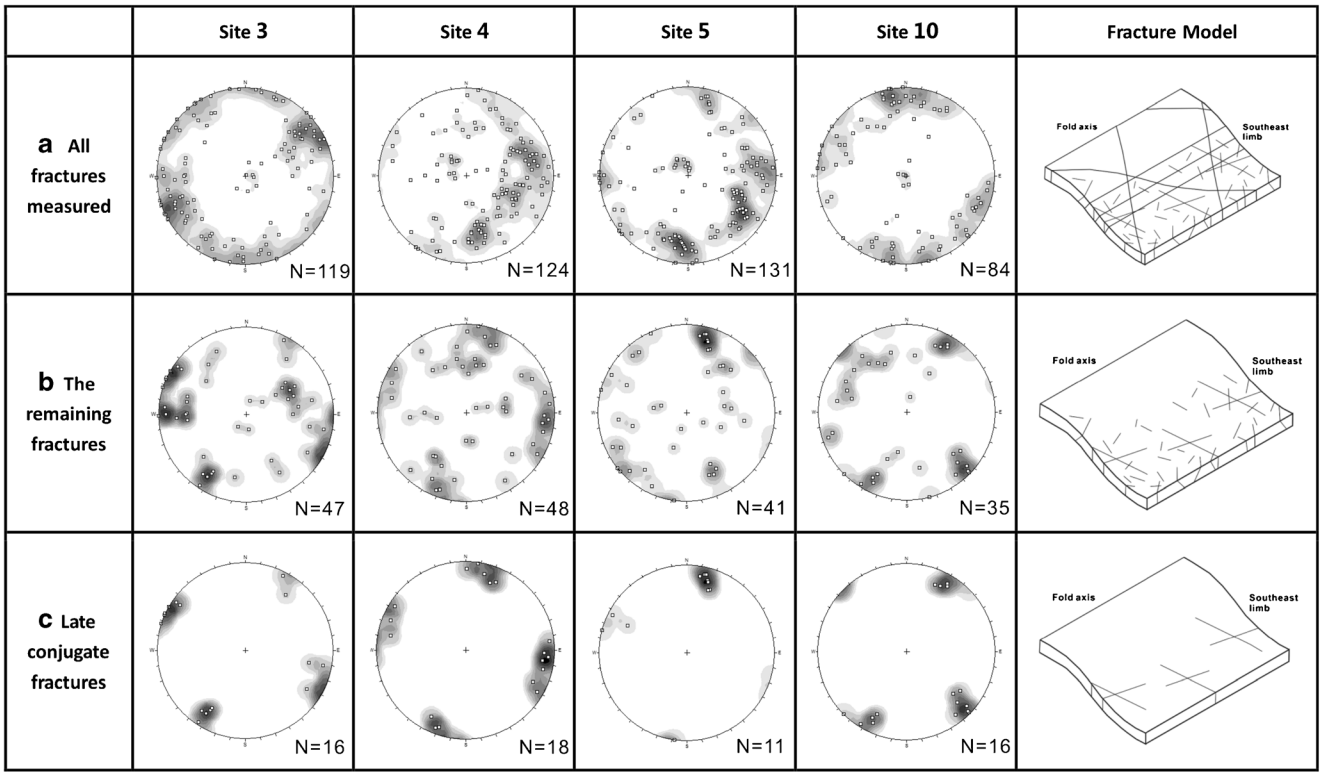

Fig. 3 The analysis of fracture fabrics was based on the removal of fractures from different periods. **a** Among all of the fractures, three sets were predominant. **b** Fracture fabrics after removing the predominant fracture sets; the remaining poles are relatively scattered. **c** In the remaining fractures, two sets of fractures are widespread in the southeast limb of the Pingluoba anticline. *N* represents the number of fracture poles in the stereonet

account for more than 60 % of the total number, and concentrate as clusters in the polar stereonet. Generally, the most intense tectonic event would be expected to result in the development of the primary fractures among the fracture sets. Therefore, we assumed that these fractures were formed during the development of the Pingluoba anticline, i.e., during the principal deformation period in the area. On the basis of fracture characteristics given below, we suggest that these three fracture sets were formed during the development of the Pingluoba anticline as a set of conjugate shear fractures (N and E sets) and as a tensile fracture set (NE).

After removing these three sets of fractures from the fracture fabrics, the remaining poles of fractures are relatively scattered (Fig. 3b). Nevertheless, two correlative sets are present in the southeast limb of the Pingluoba anticline. Although the number of fractures of the two sets is relatively smaller, they are still considered as fractures sets under structural stress control rather than part of the background random scatter because the two sets are universally developed at all the four sites. These two fracture sets, with consistent strike directions to the NNE and SEE, predominate in the remaining fracture fabrics and are present in pairs at the sites (Fig. 3c). These two sets of fractures are considered to have developed as a conjugate set of shear fractures and therefore formed in the same period and under the same stress (see next section). These fractures are relatively few in number and consequently are easy to neglect during field observations. These two fracture sets were then removed from the fracture fabrics; the results revealed that no more correlative sets were observable. Therefore, we inferred that the fractures in the area were developed during two periods. But the sequence of fracture development requires more analysis. Fractures, formed in different periods, usually have specific orientations and spatial relationship to beddings in accordance with the deformation mode of strata in each period, which provides evidence for identification of development sequence of fractures. Moreover, because pre-existing fractures would affect the distribution and concentration of stress in subsequent deformation, the development of late-formed factures would be affected by pre-existing fractures and show different characteristics in fracture features such as length, extending, and distribution. Therefore, fracture features and orientations were then analyzed and compared to determine the development sequence of fractures.

Fracture feature analysis

Among the three predominant fracture sets obtained from the fracture fabrics (Fig. 4), the N- and E-striking sets are considered as plane conjugate shear fractures (Fig. 4b). According to field observations, these fractures are perpendicular to bedding and have straight extension, smooth surfaces, small apertures, steps and slickenlines, and no mineral fillings. The

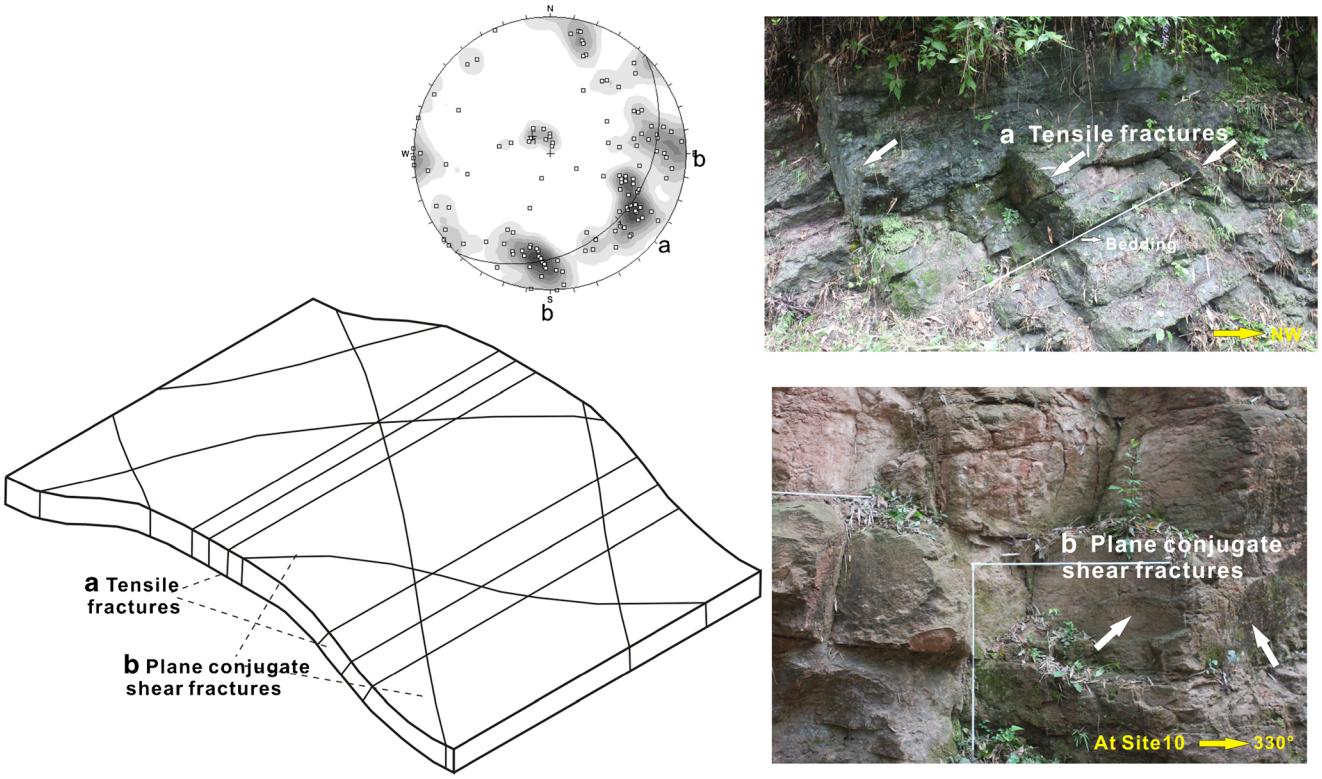

Fig. 4 Field photos and model of fractures developed during fold evolution. A set of tensile fractures which are perpendicular to bedding and strike parallel to fold axis (**a**), and two sets of plane conjugate shear fractures (**b**) which are also perpendicular to bedding are mainly formed

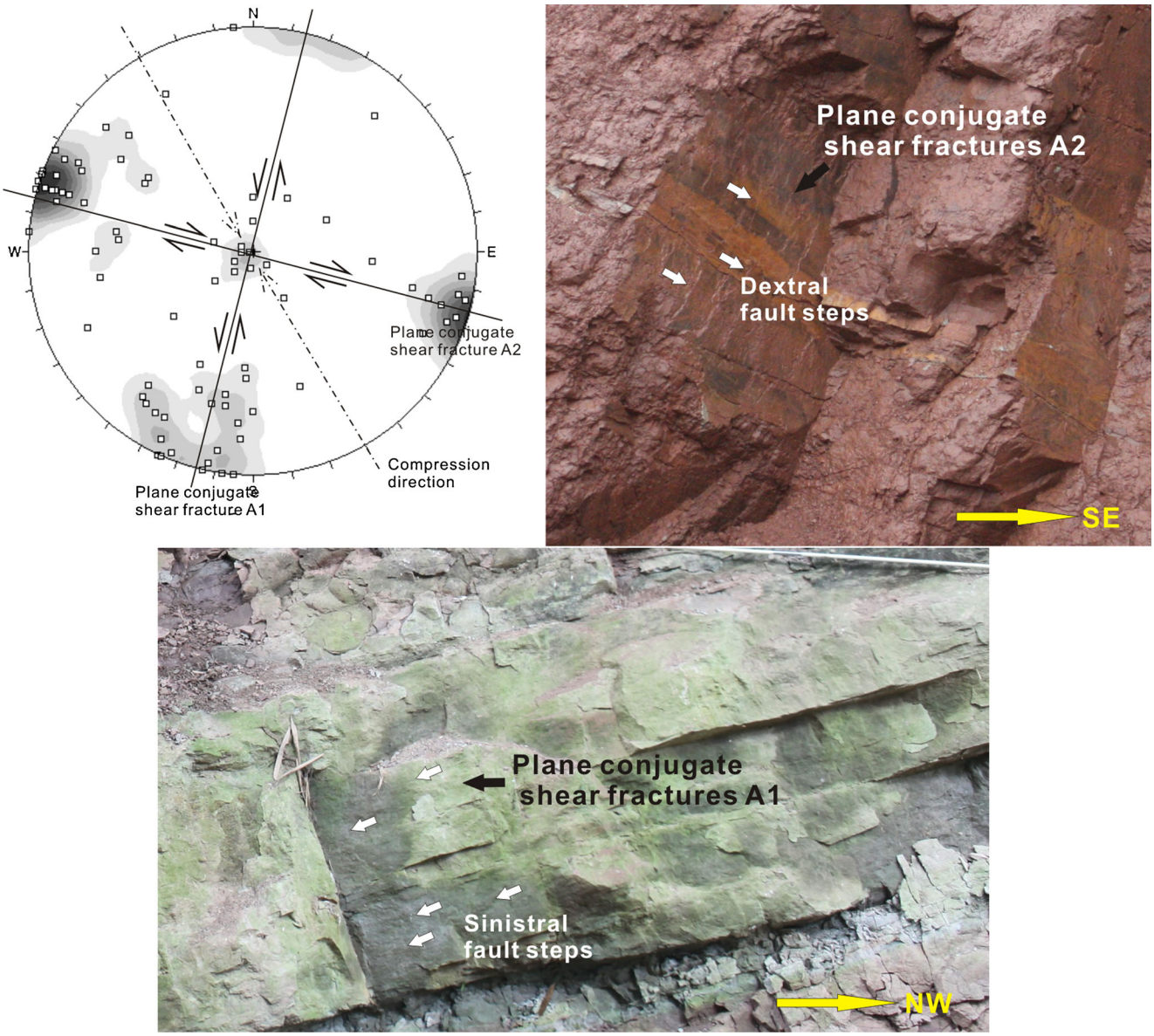

Fig. 5 Steps and slickenlines of the plane conjugate shear fractures suggest that the N-S striking fractures are sinistral and the E-W striking fractures are dextral. The plane conjugate shear fractures suggest a northwest compression

movement direction indicated by the steps is perpendicular to the intersecting line of the two fractures and strike of strata. The steps and slickenlines show that the N- and the E-striking fractures, which are sinistral and dextral respectively, have typical feature of conjugate shear fractures (Fig. 5). The two fracture sets are formed under horizontal compression at the initial stage of folding, and their acute bisector follows the compression that controlled the formation of the anticline (Fischer and Wilkerson 2000; Guiton et al. 2003; Ismat 2008). The other northeast-striking set is perpendicular to bedding planes and parallel to the strike of the strata and fold axis of the Pingluoba anticline. These fractures have rough surfaces, more-sinuous extensions, no steps or slickenlines, and larger apertures than the plane conjugate shear fractures (Fig. 4b). Orientations and these features suggest that these fractures were formed under the extensional stress induced by the bending deformation of strata during folding; the bending axis of strata is parallel to the fold axis, so the extensional stress is perpendicular to the fold axis and parallel to the regional compression (Ramsay and Huber 1987; Price and Cosgrove 1990; Lemiszki et al. 1994; Engelder and Peacock 2001; Smart et al. 2009). The genetic interpretations of these fracture sets show clear correlation with features of the Pingluoba anticline, so these fractures are believed to have developed during the evolution of Pingluoba anticline.

The other two fracture sets, developed in another period, are mainly present in the southeast limb of Pingluoba anticline. The features of these fractures are similar to those of

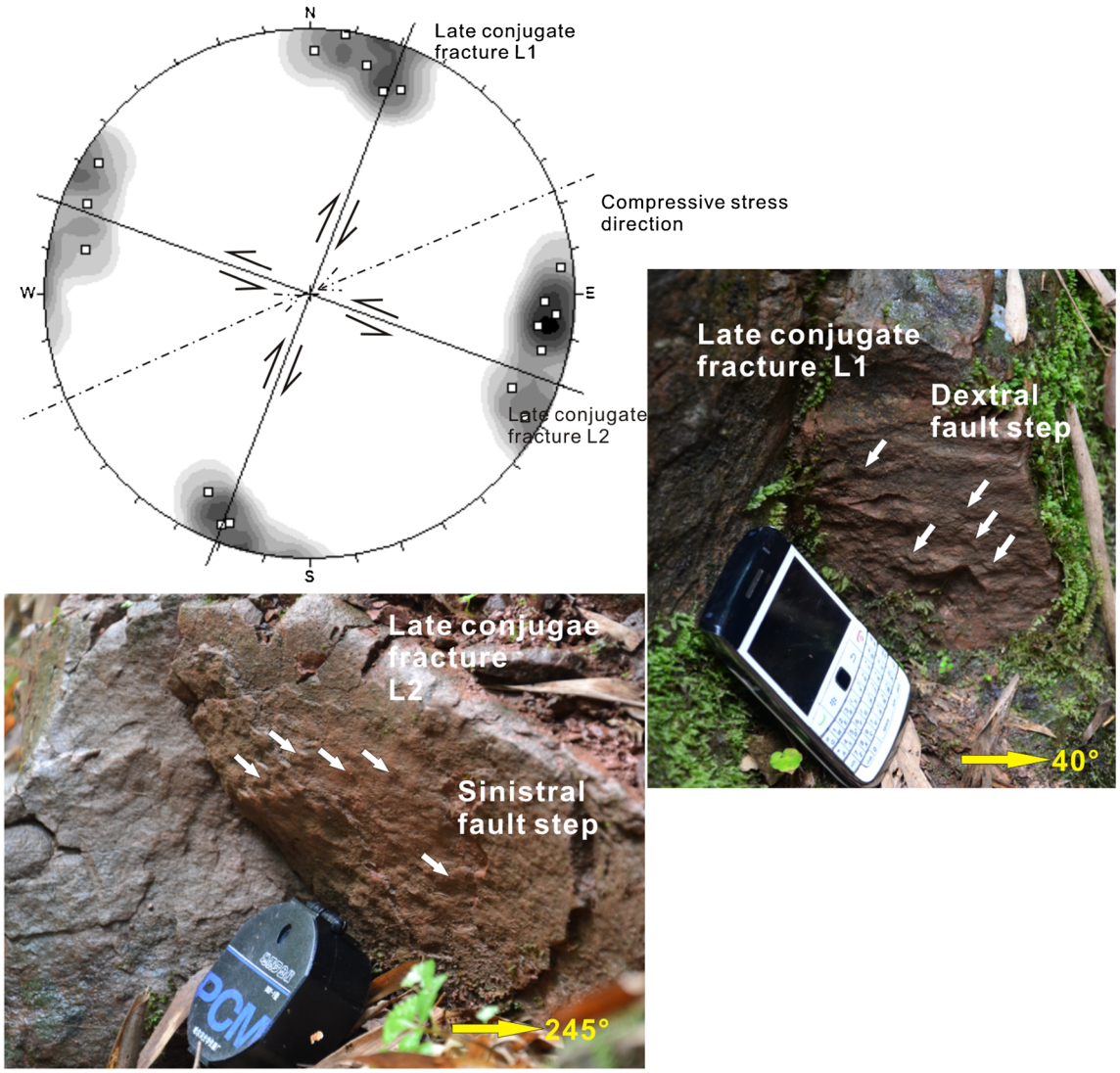

Fig. 6 At site 4, steps and slickenlines of the late conjugate shear fractures suggest that the SEE-striking fractures are sinistral and the NNE-striking fractures are dextral. The acute bisector indicates a nearly E-W striking compression

the plane conjugate shear fractures: they display straight extensions, smooth surfaces, steps and slickenlines on the fracture surfaces, and no mineral fillings. The steps and slickenlines indicate that the SEE- and NNE-striking and fractures are sinistral and dextral, respectively (Fig. 6). The most significant difference between these and the fold-related fractures is that at sites with inclined strata the two sets are both nearly vertical, rather than perpendicular to bedding. The three fold-related fracture sets in the study area are all perpendicular to bedding. Fractures that developed before folding are expected to be perpendicular to bedding; or the orientations would not be expected to be consistent among different sites because of the different directions and magnitudes of strata deformation. This finding suggests that these two sets were developed under a later compression, after the folding of the Pingluoba anticline. For this reason, the two fracture sets are provisionally categorized as late conjugate shear fractures.

In addition to the spatial relationship with bedding, other evidence also shows that the two late conjugate shear fracture sets were developed relatively late and were affected by pre-existing structures. The plane conjugate shear fractures, which were initially developed in homogeneous rock under compression, are long and straight, whereas the late conjugate fractures are shorter, and smaller in number, and orientations of some individual fractures display obvious deviation. These differences suggest that development of the late conjugate fractures was affected by pre-existing fractures. On the other hand, the late conjugate shear fractures are only present in the sandy mudstone of the Guankou Formation in the southeast limb of the anticline but not in the lithic sandstones of the Jiaguan Formation. This finding suggests that the stress that induced the development of

the late conjugate fractures was a result of relatively weak compression, whereas the principal deformation in the area was caused by a stronger compressive stress that was able to fracture stronger rocks.

Stress field analysis based on fractures

The directions of the fold-related shear fractures and tensile fractures were used to estimate the stress direction during the principal deformation period. In the plane conjugate shear fractures, the N- and E-striking fractures are, respectively, sinistral and dextral. Their acute bisector indicates that the compressive stress strikes NW (Fig. 5). The strike of the bending axis of strata is parallel to the tensile fractures and perpendicular to the regional compressive stress. So a NW-SE striking compressive stress can also be indicated by the northeast striking tensile fractures.

In the late conjugate fractures, the SEE- and NNE-striking fractures are sinistral and dextral, respectively. Their acute bisector indicates that the compression is oriented nearly E-W (Fig. 6). Based on the sequence of fracture development, an E-W compression was applied after the formation of Pingluoba anticline and resulted in the later structural superposition in the area. The Qiongxi belt in the eastern part of the area was formed under E-W compression and developed after the Pingluoba anticline (Jia et al. 2007, 2009). The development period of the Qiongxi belt is consistent with that of the late conjugate fractures. The two compressive stresses, which induce the formation of the Qiongxi belt and the late conjugate fractures, respectively, are consistent in direction and timing and are therefore considered to have developed under the same stress.

Considering the discussion above, the strike of compressive stress in the area had changed from NW-SE to E-W in two structural periods. This change is consistent with the development

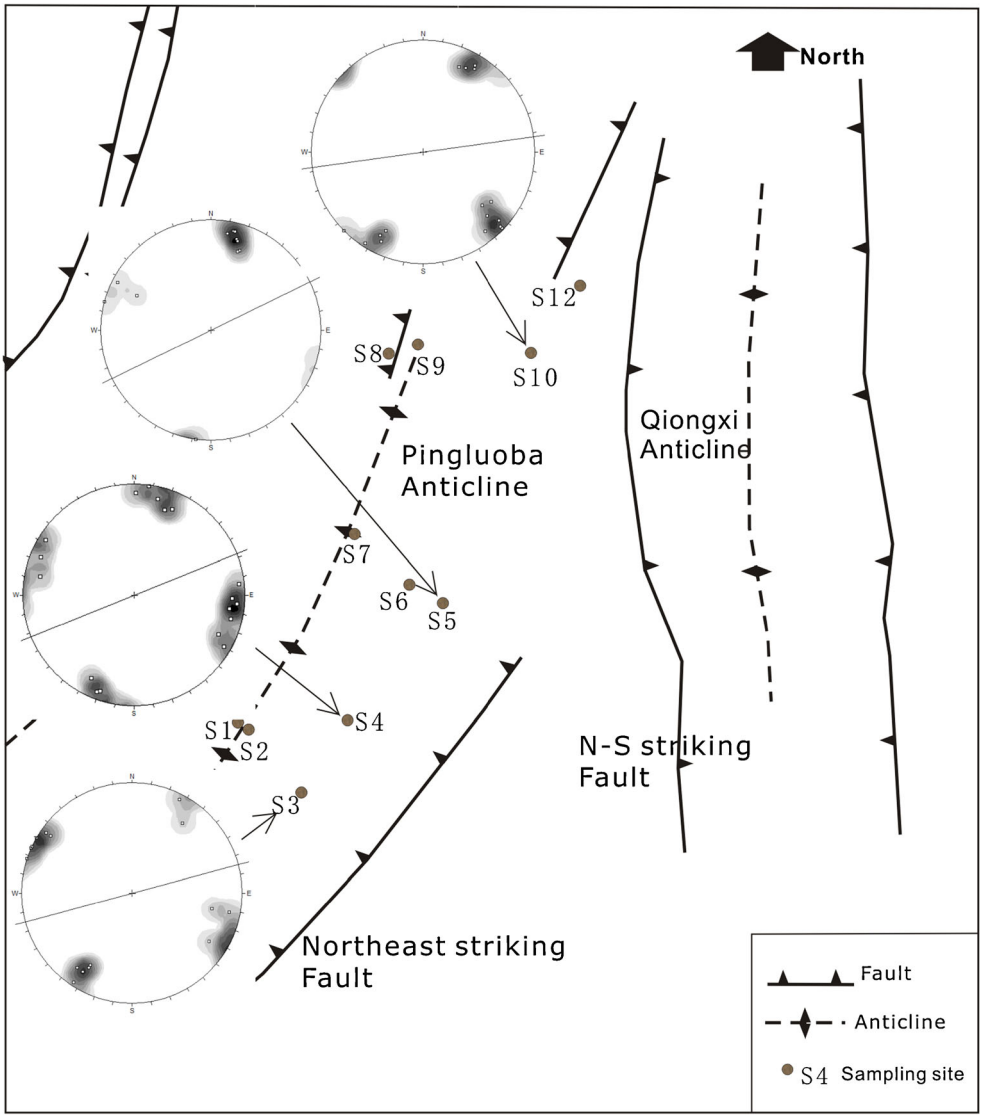

Fig. 7 Compression directions indicated by the late conjugate fractures in the southeast limb of the Pingluoba anticline. The E-W stress has rotated to NEE direction

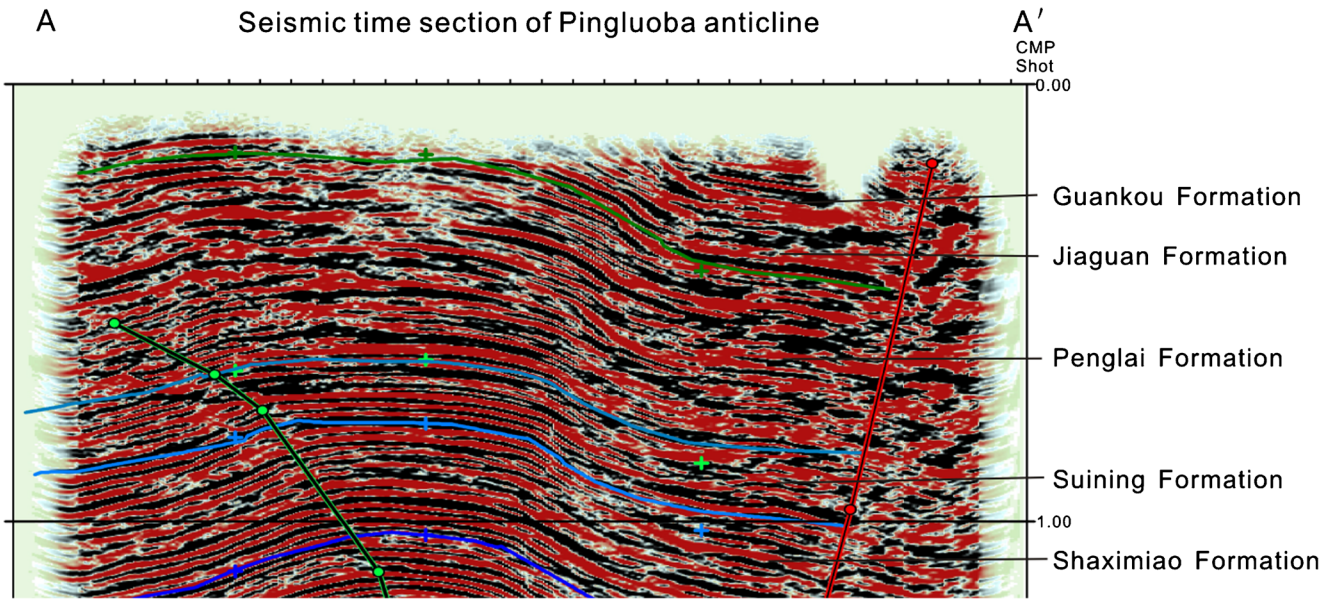

Fig. 8 Seismic time profile in the Pingluoba anticline. Parameters of the FEM model, such as fold shape, fault dip, and formation thickness, are obtained based on the profile

sequence of the Pingluoba and Qiongxi anticlines. The consistency also suggests that the indicator fractures of each period, which are obtained from the analysis of fracture fabrics and features, are correct and representative.

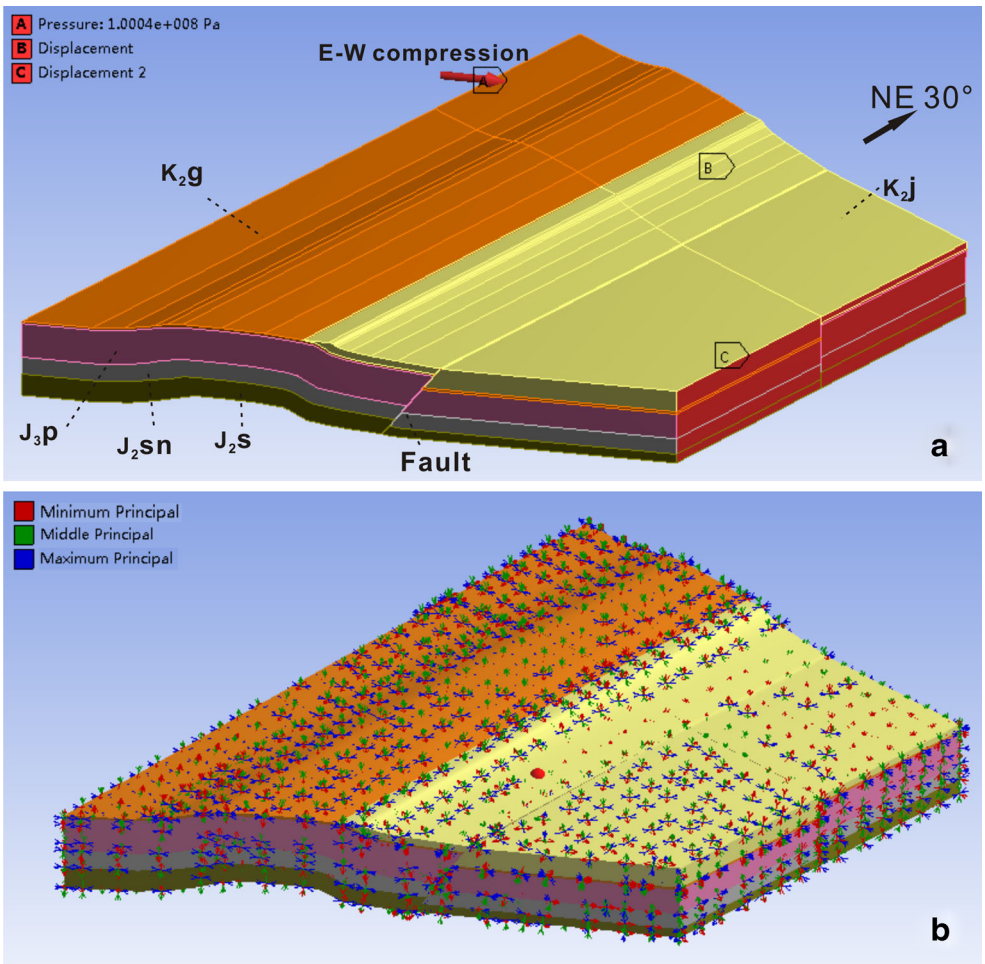

Fig. 9 On the west side of the model, a compressive stress striking E-W is applied; on the east side, the horizontal displacement is constrained as zero. The front boundary is set parallel to the compression stress to eliminate the boundary effect (**a**). The simulation result of the principal stresses of the model (**b**)

Table 1 The Young's modulus and Poisson's ratio of the materials of the formations and fault in the FEM model (Li et al. 2005)

Material	Lithology	Young's modulus (GPa)	Poisson's ratio	Density (kg/m^3)
Guankou Formation	Sandy mudstone	38.4	0.19	2,400
Jiaguan Formation	Lithic sandstone	63.1	0.183	2,710
Penglai Formation	Sandy mudstone	38.4	0.19	2,400
Suining Formation	Mudstone	33.2	0.259	2,300
Shaximiao Formation	Conglomerate	33.0	0.2	2,660
Fault		0.01	0.4	2,300

Discussion

Stress rotation and structural boundary

Further analysis of the stress directions reveals that a small angular difference exists between the stress direction indicated by the late conjugate fractures and the regional E-W compression. In the southeast limb of the Pingluoba anticline, the general stress strikes N60°-70°E at site 3, site 4, and site5, although small variations exist, while the stress strikes N85°E at site 10, which is located in the plunging crown of the fold and far from the NE-striking fault (Fig. 7). The NEE direction stress is close to the regional E-W compression but has rotated counterclockwise. The variation in strikes of these fractures is consistent across these sites, suggesting that the stress rotation is indeed present. Although the angular difference exists, the consistency in the development period and similarity in direction support the fact that the NEE stress results from the regional E-W compression.

The reason for the stress rotation was further analyzed. The main difference between the Pingluoba anticline, where the stress is rotated, and the N-S striking Qiongxi belt is that the Pingluoba anticline and its related structures were already present when the E-W compression stress was applied. Previous studies have revealed that structural boundaries, such as faults, can affect the direction and magnitude of stress (e.g., Pollard and Segall 1987; Homberg et al. 1997; Kattenhorn et al. 2000; García-Navarro and Fernández 2010). Therefore, it is inferred that the 20° to 30° counterclockwise rotation in the stress direction was induced by the structural boundary, i.e., the Pingluoba belt, which consists of a NE-striking thrust fault and an anticline. To verify this inference, a finite element

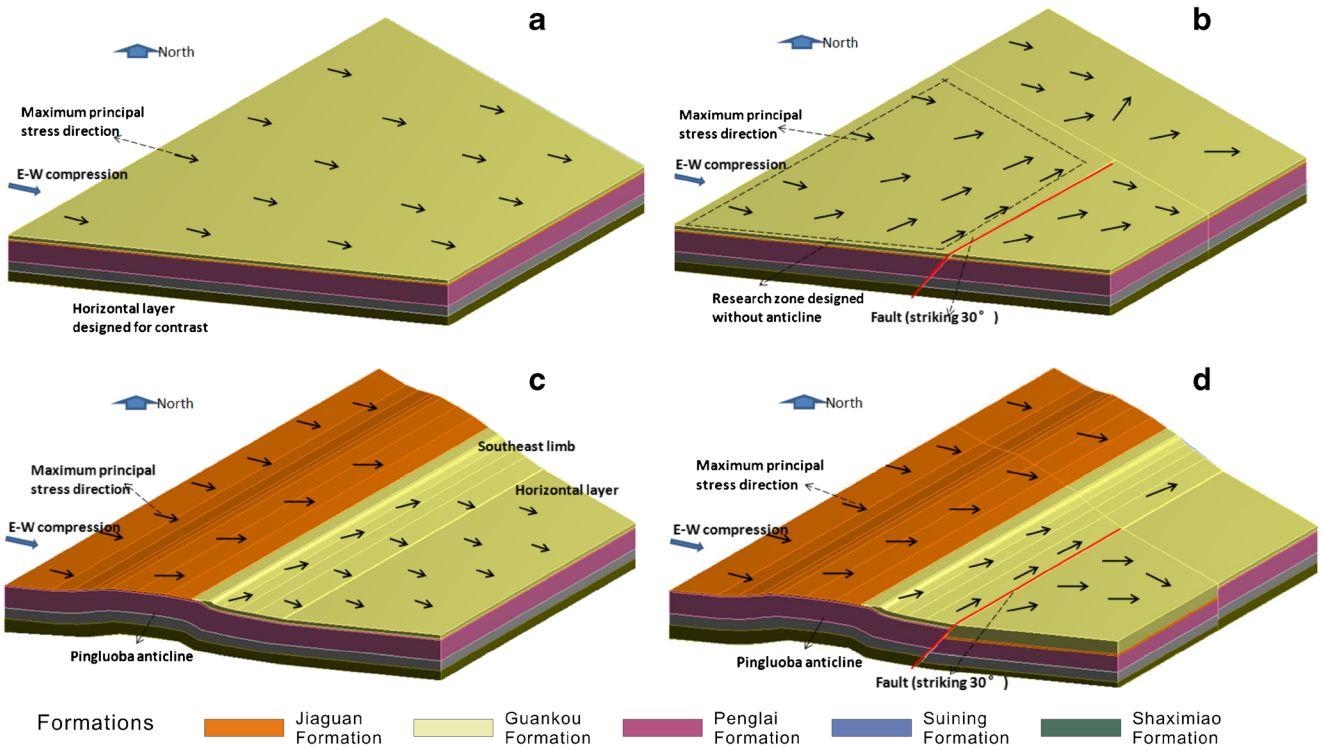

Fig. 10 Four FEM models were designed to simulate the stress distributions and analyze the controlling factors (The direction of maximum principal stress is simplified as a *single arrow* to make the figure clear): **a** The stress direction in horizontal strata. **b** The rotation of stress direction near the fault. **c** The rotation of stress direction inside the anticline. **d** The distribution of stress direction in the Pingluoba belt

method (FEM) model with settings analogous to the Pingluoba belt was developed to simulate the stress direction under the effects of the anticline and fault.

Finite element simulation

Based on the recognition of the regional tectonic evolution, the northeast-striking Pingluoba belt experienced an E-W compression after its development. Therefore, in our FEM simulation, a three-dimensional model of the Pingluoba anticline was developed first and then an E-W compression stress was applied to simulate the changes in stress direction in the study area.

The parameters of the three-dimensional FEM model were set comparable to the natural structures of the Pingluoba belt, including the formation thickness, the formation sequence, the strike and dip of the fault, the shape of the anticline, the positions of fault and anticline, and the horizontal length of each unit. The thickness of each formation was calculated based on the seismic time section (A-A' in Fig. 1) and logging data, and the dip of fault was determined by the ratio of the horizontal length and depth in the section (Fig. 8). In the model, the mechanical parameters of formations in a neighboring area in the east Sichuan basin (Li et al. 2005) were used to represent the corresponding formation in the study area (Table 1). Each formation was assigned a distinctive color in the model. The simulated fault consisted of material with a low Young's modulus and a high Poisson's ratio, in accordance with previous parameters-reducing simulation method of fault zone (Zou et al. 2001; Yang et al. 2006). The contact relationship between the fault and adjacent formations was set as bonded. On the west side of the model, an E-W compressive stress was applied, which equaled 1×10^8 Pa; on the east side, the horizontal displacement was constrained as zero. The front boundary was set parallel to the compression stress to eliminate the boundary effect, and the back boundary was not constrained (Fig. 9a). In the study, the setup and simulation of the FEM model were performed in the static structural module of the software ANSYS Workbench 12.0.

To fully understand the controlling factors of stress rotation in the Pingluoba belt, four FEM models were built: (A) a model with horizontal strata (Fig. 10a), (B) a model with horizontal strata with a northeast-striking fault (Fig. 10b), (C) a model with an anticline (Fig. 10c), and (D) a model with a fault and an anticline, which is analogous to the Pingluoba belt (Fig. 10d).

The simulation suggests that the stress direction rotates differently between the four models. In model A, which lacks pre-existing structures, the maximum principal stress maintains the original E-W direction (Fig. 10a). In model B, which includes a northeast striking fault, the stress direction begins to gradually rotate counterclockwise to an NEE direction and finally becomes parallel to the fault (Fig. 10b). In model C, which includes northeast-striking anticline, the stress rotates to an NEE direction in the southeast limb of the anticline and changes back to E-W away from the anticline axis (Fig. 10c). In model D, which includes settings analogous to the Pingluoba anticline, the stress strikes NEE; the rotation is greater than that of models B and C; in the southeast limb, the stress direction rotates 30° counterclockwise (Fig. 10d).

The counterclockwise rotation of stress direction observed in the southeast limb is consistent with the stress change indicated by the late conjugate shear fractures. The simulation also suggests that the presence of the fault and anticline would induce the rotation of stress as a combined structural boundary if the stress is oblique to them.

Conclusion

1. This paper identifies the period of fracture development based on the analysis of fracture fabrics and features. The analysis of fracture fabrics suggests that two periods of fracturing occurred in the study area. Combined with fracture features, the fractures are confirmed to be related to the development of the Pingluoba anticline and a subsequent compression.
2. This fracture analyzing method, based on specific field measurement and fracture fabrics analysis, is especially suitable in areas where the abutting relationships of complex fractures are unclear and insufficient.
3. The stress direction indicated by the late conjugate fractures suggests that the regional E-W compressive stress rotates 20–30° counterclockwise because of structural boundaries, i.e., the pre-existing Pingluoba belt. Our simulation using an FEM model indicates that the presence of a fault and anticline leads to a counterclockwise rotation of the stress direction, and the rotated stress is compatible with the stress direction indicated by the fractures.

Acknowledgments The paper is supported by the Chinese National Science and Technology Major Project (2011ZX05009-001). We benefited from extensive discussion with our colleagues in the Department of earth science, University of Zhejiang. We would like to thank Structural Research Centre of Oil & Gas Bearing Basin of Chinese Ministry of Education for supporting this work and providing the explanation profiles of seismic reflection time cross sections.

References

Bellahsen N, Fiore P, Pollard DD (2006) The role of fractures in the structural interpretation of Sheep Mountain Anticline, Wyoming. J Struct Geol 28:850–867

Blenkinsop TG (2008) Relationships between faults, extension fractures and veins, and stress. J Struct Geol 30(5):622–632

Burchfiel BC, Chen Z, Liu Y, Royden LH (1995) Tectonics of the Longmen Shan and adjacent regions, central China. Int Geol Rev 37:661–735

Deng B, Liu SG, Jansa LB, Cao JX, Cheng Y, Li ZW, Liu S (2012) Sedimentary record of Late Triassic transpressional tectonics of the Longmenshan thrust belt, SW China. J Asian Earth Sci 48:43–55

Diabat A (2013) Fracture systems of granites and Quaternary deposits of the area east of Aqaba: indicators of reactivation and neotectonic activity. Arab J Geosci 6(3):679–695

Dirks P, Wilson CJL, Chen S, Luo Z, Lin S (1994) Tectonic evolution of the NE margin of the Tibetan Plateau: evidence from the central Longmen Mountains, Sichuan Province, China. J SE Asian Earth Sci 9:181–192

Dyer R (1988) Using joint interactions to estimate paleostress ratios. J Struct Geol 10:685–699

Engelder T, Peacock DCP (2001) Joint development normal to regional compression during flexural-flow folding: the Lilstock buttress anticline, Somerset, England. J Struct Geol 23:259–277

Eyal Y, Gross MR, Engelder T, Becker A (2001) Joint development during fluctuation of the regional stress field in southern Israel. J Struct Geol 23(2–3):279–296

Eyal Y, Osadetz KG, Feinstein S (2006) Evidence for reactivation of Eocene joints and pre-Eocene foliation planes in the Okanagan core-complex, British Columbia, Canada. J Struct Geol 28:2109–2120

Fischer MP, Wilkerson MS (2000) Predicting the orientation of joints from fold shape: results of pseudo three-dimensional modeling and curvature analysis. Geology 28:15–18

García-Navarro E, Fernández C (2010) Palaeostress perturbations near the El Castillo de las Guardas fault (SW Iberian Massif). J Struct Geol 32(5):693–702

Ghosh SK, Ramberg H (1968) Buckling experiments on intersecting fold patterns. Tectonophysics 5:89–105

Ghosh SK, Mandal N, Khan D, Deb SK (1992) Modes of superposed buckling in single layers controlled by initial tightness of early folds. J Struct Geol 14:381–394

Guiton M, Sassi W, Leroy Y, Gauthier B (2003) Mechanical constraints on the chronology of fracture activation in the folded Devonian sandstone of the western Moroccan Anti-Atlas. J Struct Geol 25:1317–1330

Homberg C, Hu JC, Angelier J, Bergerat F, Lacombe O (1997) Characterization of stress perturbations near major fault zones: insights from 2-D distinct-element numerical modeling and field studies (Jura Mountains). J Struct Geol 19:703–718

Ismat Z (2008) Folding kinematics expressed in fracture patterns: an example from the Anti-Atlas fold belt, Morocco. J Struct Geol 30:1396–1404

Ismat Z, Mitra G (2005) Folding by cataclastic flow: evolution of controlling factors during deformation. J Struct Geol 27(12):2181–2203

Jia D, Wei GQ, Chen ZX, Li BL, Zeng Q, Yang G (2006) Longmen Shan fold-thrust belt and its relation to the western Sichuan Basin in central China: new insights from hydrocarbon exploration. AAPG Bull 90(9):1425–1447

Jia QP, Jia D, Zhu AL, Chen ZX, Hu QW, Luo L, Zhang YY, Li YQ (2007) Active tectonics in the Longmen thrust belt to the eastern Qinghai-Tibetan Plateau and Sichuan Basin: evidence from topography and seismicity. Chin J Geol 42:31–44 (in Chinese with English abstract)

Jia QP, Jia D, Luo L, Chen ZX, Li YQ, Deng F, Sun SS, Li HB (2009) Three-dimensional evolutionary models of the Qiongxi structures, southwest Sichuan Basin, China: evidence from seismic interpretation and geomorphology. Acta Geol Sin 83(2):372–385

Jin WZ, Tang LJ, Yang KM, Wan GM, Lü ZZ (2010) Segmentation of the Longmen Mountains thrust belt, Western Sichuan Foreland Basin, SW China. Tectonophysics 485:107–121

Kattenhorn SA, Aydin A, Pollard DD (2000) Joints at high angles to normal fault strike; an explanation using 3-D numerical models of fault perturbed stress fields. J Struct Geol 22:1–23

Lemiszki PT, Landers JD, Hatcher RD (1994) Controls on hinge-parallel extension fracturing in single-layer tangential-longitudinal strain folds. J Geophys Res 99:22027–22041

Li ZW, Luo YH, Liu SG, Gong CM, Shan YM, Liu WG, Liu S, Yong ZQ, Sun W (2005) The experimental analysis of mechanical properties of compact reservoir rocks under formation conditions, northeast of Sichuan basin, China. J Mineral Petrol 25(4):52–60 (in Chinese with English abstract)

Liu S (2006) Structural characteristics of the thrust fold of foreland—a case study of the thrust fold at Micang and Longmen Mountains. Institute of Geology, China Earthquake Administration, Beijing, pp 29–31 (in Chinese with English Abstract)

Memarian H, Fergusson CL (2003) Multiple fracture sets in the south-eastern Permian-Triassic Sydney Basin, New South Wales. Aust J Earth Sci Int Geosci J Geol Soc Aust 50(1):49–61

Mynatt I, Seyum S, Pollard DD (2009) Fracture initiation, development, and reactivation in folded sedimentary rocks at Raplee Ridge, UT. J Struct Geol 31:1100–1113

Olson JE (1997) Natural fracture pattern characterization using a mechanically-based model constrained by geologic data—moving closer to a predictive tool. International Journal of Rock Mechanics and Mining Sciences 34: 171.e1–171.e12

Olson JE (2003) Sublinear scaling of fracture aperture versus length: an exception or the rule. J Geophys Res B9:108(2413)

Pollard DD, Aydin A (1988) Progress in understanding jointing over the past century. Geol Soc Am Bull 100:1181–1204

Pollard DD, Segall P (1987) Theoretical displacements and stresses near fractures in rocks: with applications to faults, joints, veins, dikes, and solution surfaces. In: Atkinson BK (ed) Fracture mechanics of rock. Academic Press, London, pp 277–349

Price NJ, Cosgrove JW (1990) Analysis of geologic structures. Cambridge University Press, Cambridge

Ramsay JG, Huber MI (1987) The techniques of modern structural geology 2, folds and fractures. Academic Press, London

Rawnsley KD, Rives T, Petit JP, Hencher SR, Lumsden AC (1992) Joint development in perturbed stress fields near faults. J Struct Geol 14:939–951

Smart KJ, Ferrill DA, Morris AP (2009) Impact of interlayer slip on fracture prediction from geomechanical models of fault-related folds. AAPG Bull 93(11):1447–1458

Yang YS, Shen XH, Zou LJ (2006) Finite element simulation on control effect of deformation stress field of folds on fractures. Bull Sci Technol 22(5):616–621 (in Chinese with English abstract)

Zou LJ, Shen XH, Zhang H, Fang DJ (2001) The application of F_n index method in fracture distribution pattern of complex structure. J Zhejiang Univ (Sci Ed) 28(1):112–118 (in Chinese with English abstract)